Supplementary Materials & Methods

Pathogenic cysteine removal mutations in FGFR extracellular domains stabilize receptor dimers and perturb the TM dimer structure

Sarvenaz Sarabipour and Kalina Hristova

Department of Materials Science and Engineering

Johns Hopkins University, Baltimore, MD 21212

Materials and Methods.

Plasmids. The pRSETB-YFP and pRSETB-mCherry plasmids were gifts from Dr. M. Betenbaugh (Johns Hopkins University, Baltimore, MD) and Dr. R.Tsien (University of California, San Diego), respectively. The plasmids encoding human wild-type FGFR1 and FGFR2 in the pRK5 vector were obtained from Dr. M. Mohammadi, NYU. The plasmid encoding human wild-type FGFR3 was a gift from Dr. D. J. Donoghue, UCSD. All the plasmids used for mammalian expression were constructed in the pcDNA 3.1(+) vector (Invitrogen). All primers were purchased from Invitrogen.

The cloning procedures for the plasmids encoding for wild-type full-length and truncated human FGFR1, FGFR2 and FGFR3 receptors has been published previously [1,2]. The full-length receptors were tagged with either YFP or mCherry (a FRET pair) at their C-termini, attached via a flexible GGS linker. The truncated EC+TM FGFR receptors consisted of the extracellular (EC) domains, the transmembrane (TM) domains, a flexible $(GGS)_5$ linker and the fluorescent proteins. This type of attachment of the fluorescent proteins to the TM domains has been shown to not prevent the close interactions of the TM domains, and had no measurable effect on dimerization propensities [3].

For this work, we created 12 plasmid constructs by introducing single amino acid mutations in full length and truncated FGFR1, FGFR2 and FGFR3 using the QuikChange® II XL Site-Directed Mutagenesis Kit (Stratagene, CA) (see Figure 1). In particular, we created the C178S mutation in the FGFR1 EC+TM-$(GGS)_5$-YFP, FGFR1 EC+TM-$(GGS)_5$-mCherry, FGFR1-(GGS)-YFP and FGFR1-(GGS)-mCherry plasmids. We introduced the C342R mutation into the FGFR2 EC+TM-$(GGS)_5$-YFP, FGFR2 EC+TM-$(GGS)_5$-mCherry, FGFR2-(GGS)-YFP and FGFR2-(GGS)-mCherry plasmid constructs. Finally, we created the C228R mutation in the FGFR3 EC+TM-$(GGS)_5$-YFP, FGFR3 EC+TM-$(GGS)_5$-mCherry, FGFR3-(GGS)-YFP and FGFR3-(GGS)-mCherry plasmid constructs.

Cell culture and transfection. Chinese Hamster Ovary (CHO) cells and Human Embryonic Kidney (HEK) 293 T cells were cultures at 37 ˚C with 5% CO_2 for 24h. Transfection was carried out with 3-7 μg of DNA, using Fugene HD transfection reagent (Roche Applied Science), following the manufacturer's protocol. Cells were co-transfected with genes encoding either YFP or mCherry-tagged full-length or truncated receptors. No staining for FGFR1, FGFR2 or FGFR3 was ever observed in CHO and HEK293T cells in Western blotting experiments, unless the cells were transfected.

Production of mammalian plasma membrane vesicles. The plasma membrane-derived vesicles closely resemble the cellular plasma membranes in lipid composition but lack cytoplasmic content [4]. Vesiculation was performed with a chloride salt vesiculation buffer consisting of 200 mM NaCl, 5 mM KCl, 0.5 mM $MgSO_4$, 0.75 mM $CaCl_2$, 100 mM bicine and protease inhibitor cocktail (Complete mini EDTA-free tabs, Roche Applied Science) adjusted to PH of 8.5 [5]. CHO cells were rinsed twice with 30% PBS (pH 7.4), and incubated with 1 mL of chloride salt vesiculation buffer overnight at 37 °C. A large number of vesicles were produced after 12 h. The vesicles were transferred into 4-well Nunc Lab-Tek II chambered coverslips prior to imaging.

QI-FRET Image Acquisition. Vesicles were imaged using a Nikon Eclipse confocal laser scanning microscope using a 60× water immersion objective. All the images were collected and stored at a 512 × 512 resolution. Three different scans were performed for each vesicle: (1) excitation at 488 nm, with a 500-530 nm emission filter (donor scan); (2) excitation at 488 nm, with a 565-615 nm emission filter (FRET scan); and (3) excitation at 543 nm, with a 650 nm longpass filter (acceptor scan). The bleaching of the fluorescent proteins was minimized through the use of ND8 filters when exciting with the 488 nm laser, and low pixel dwell time (1.68 μs). Images of a vesicle expressing donor and receptor labeled FGF receptors are shown in Figure 2.

QI-FRET data Analysis: Methodology and Protocol. The quantitative imaging FRET method has been described previously as a step-by-step protocol [6]. This method yields both the FRET efficiency, and the concentrations of donors and acceptors, thus allowing us to collect binding curves and determine the dimerization free energy for membrane receptors.

For concentration calibrations, purified solutions of YFP and mCherry were produced [7] and concentrated in vesiculation buffer. They were imaged in the donor, acceptor and FRET channels prior to each experiment to determine the calibration constants for the donor and the acceptor, i_D and i_A, and the bleed-through coefficients for the donor and the acceptor, β_D and β_A as previously described [8]. Vesicles loaded with a soluble linked YFP-mCherry protein were also imaged in the three channels to obtain the gauge factor G_F [8].

A large number of vesicles (200 to 500), expressing the FGF receptors tagged with donors and acceptors, were imaged using the same settings as the calibration experiments above. The acceptor concentrations in each vesicle, C_A, was calculated according to:

$$C_A = \frac{I_A}{i_A} \qquad (1)$$

Here I_A is the acceptor intensity per unit membrane area. The sensitized emission of the acceptor in each vesicle was determined as:

$$I_{SEN} = I_{FRET} - \beta_A I_A - \beta_D I_D \qquad (2)$$

Next, we calculate:

$$I_{D,corr} = I_D + G_F I_{SEN} \quad (3)$$

$$C_D = \frac{I_{D,corr}}{i_D} \quad (4)$$

where $I_{D,corr}$ is the donor intensity that would be measured in the absence of the acceptor, and C_D represents the donor concentration. The FRET efficiency, E, was calculated using eq.5:

$$E = 1 - \frac{I_D}{I_{D,corr}} \quad (5)$$

The FRET efficiency was corrected for the proximity FRET that one would expect to observe if there were no specific protein interactions, but donors and acceptors approached each other by chance within distances of 100 Å or so. This correction is required because the fluorescent proteins are confined to the two-dimensional vesicles [9-11]. The correction has been calculated for the case of RTKs tagged with fluorescent proteins, and has been verified experimentally [12]. The corrected FRET efficiency, E_D, is related to the dimeric fraction f_D via the following relationship:

$$\frac{E_D}{x_A} = f_D \text{ x I-FRET} \quad (6)$$

In equation (6), x_A is the dimeric fraction and I-FRET is the Intrinsic FRET, i.e the FRET efficiency in a dimer containing a donor and an acceptor. This is a structural parameter, which depends only on the positioning of the two fluorescent proteins in the dimer, but not on the dimerization propensity[6,13].

Based on the law of mass action, the dimeric fraction can be written as a function of the total receptor concentration, T, and the dimerization constant K according to equation 7.

$$f_D = \frac{1}{T}\left(T - \frac{1}{4K}\left(\sqrt{1+8TK} - 1\right)\right) \quad (7)$$

Substituting equation (7) into (6), we obtain:

$$\frac{E_D}{x_A} = \frac{1}{T}\left(T - \frac{1}{4K}\left(\sqrt{1+8TK} - 1\right)\right) \text{x I-FRET} \quad (8)$$

We use equation (8) to fit the measured E_D/x_A while optimizing for the two adjustable parameters: the dimerization constant K, and the value of structural parameter I-FRET.

The reported values for dissociation constant $K_{diss}=1/K$ in Table 1 are in units of receptors/μm^2. The free energy of dimerization (dimer stability) ΔG is calculated from the dimerization constant $K=1/K_{diss}$. The standard state is defined as nm^2/receptor [6], and therefore:

$$\Delta G = -RT \ln\left(\frac{10^6}{K_{diss}}\right) \quad (9)$$

In the case of 100% dimers ($f_D = 1$), equation (6) can be re-written as:

$$\text{I-FRET} = \frac{E_D}{x_A} \qquad (10)$$

Thus, measurements of E_D and x_A for each vesicle in this case allows us to directly determine the value of the Intrinsic FRET in each vesicle.

Finally, the dependence of the intrinsic FRET on the distance between the fluorescent proteins in the dimer is given by Equation 11.

$$\text{I-FRET} = \frac{1}{1+\left(d/R\right)^6} \qquad (11)$$

Here d is the distance between the acceptor and the donor in the dimer, and R is the Förster radius of the FRET pair. For YFP and mCherry, R is 53.1 Å [6].

Western blots. CHO and HEK293T cells were starved in serum-free medium for 24 h following transfection with 1-3 μg of DNA encoding full length FGFRs. They were then treated with lysis buffer (25 mM Tris-HCl, 0.5% Triton X-100, 20mM NaCl, 2 mM EDTA, phosphatase inhibitor and protease inhibitor, Roche Applied Science). Lysates were collected following centrifugation at 15,000 g for 15 min at 4 °C and loaded onto 3–8%NuPAGE®Novex®Tris–Acetatemini gels (Invitrogen, CA). The proteins were transferred onto a nitrocellulose membrane, and blocked using 5% milk in TBS. FGFR total protein levels were assessed using antibodies raised against the N-terminal epitope of FGFR3 (H-100; sc-9007), FGFR2 (H-80; sc-20735) and FGFR1 (H-76; sc-7945), all from Santa Cruz Biotechnology. This was followed by anti-rabbit HRP conjugated antibodies (W4011, Promega). The proteins were detected using the Amersham ECL detection system (GE Healthcare).

Supplemental Figures

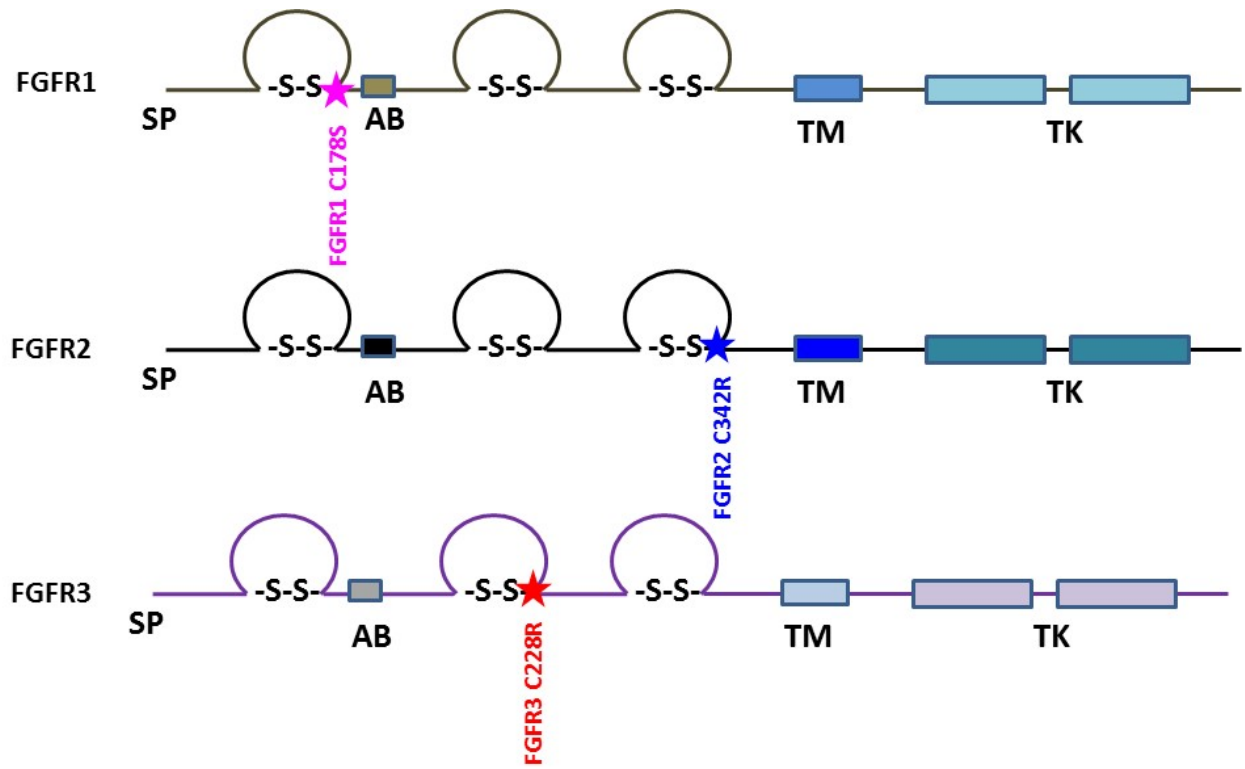

Figure S1. Schematic of FGF receptor structure and of the location of the three pathogenic mutations investigated here.

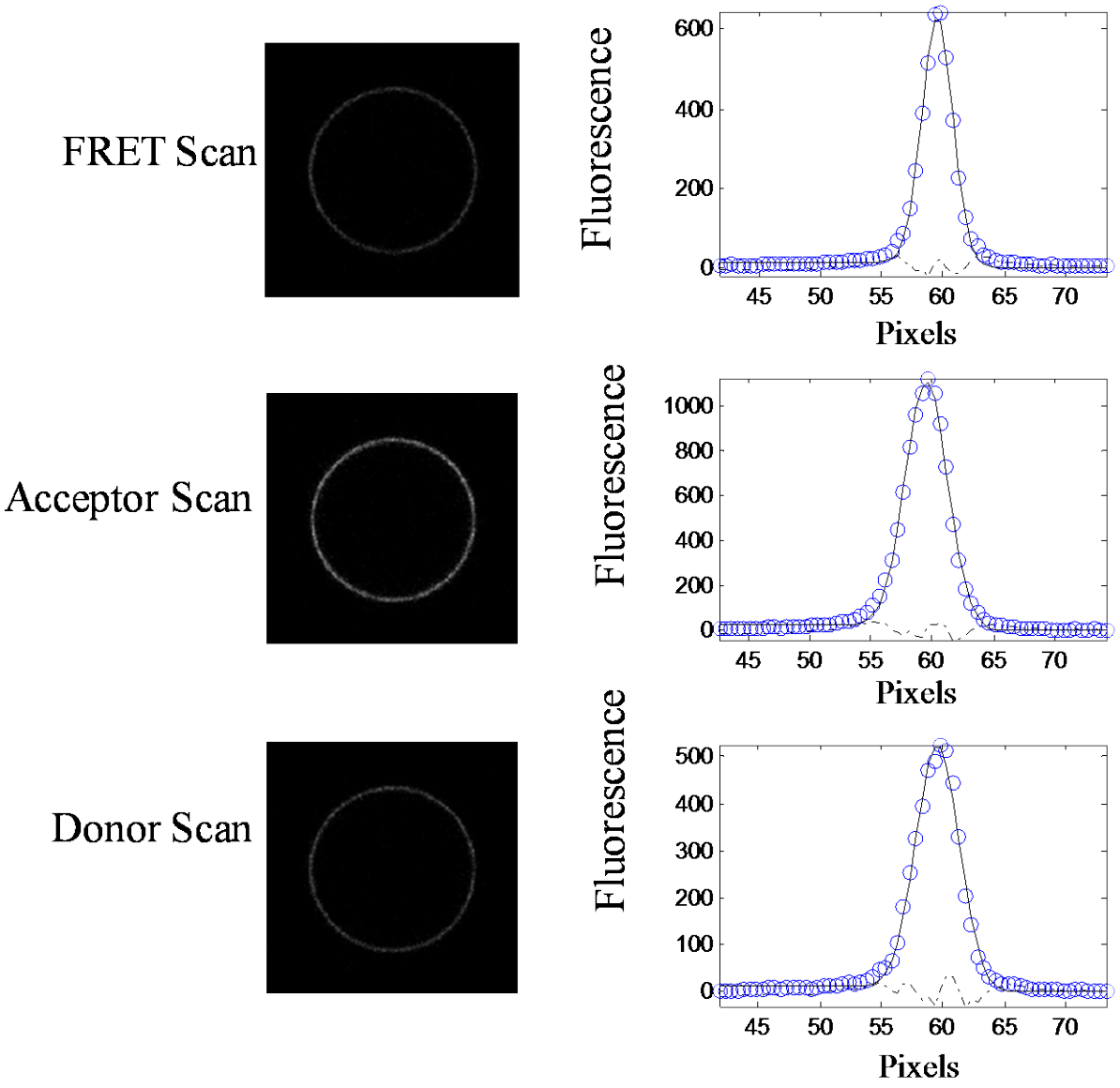

Figure S2. A vesicle, co-expressing C342R FGFR3 EC+TM-YFP and C342R FGFR3 EC+TM-mCherry, imaged and analyzed in the FRET, acceptor, and donor channels. Images were acquired with a Nikon laser scanning confocal microscope. The images are analyzed with a Matlab program that has been discussed in detail in a previous publication [6]. The intensity across the membrane (open blue symbols) is fit to a Gaussian (solid line) after background correction [6]. The residual from the fit is also shown.

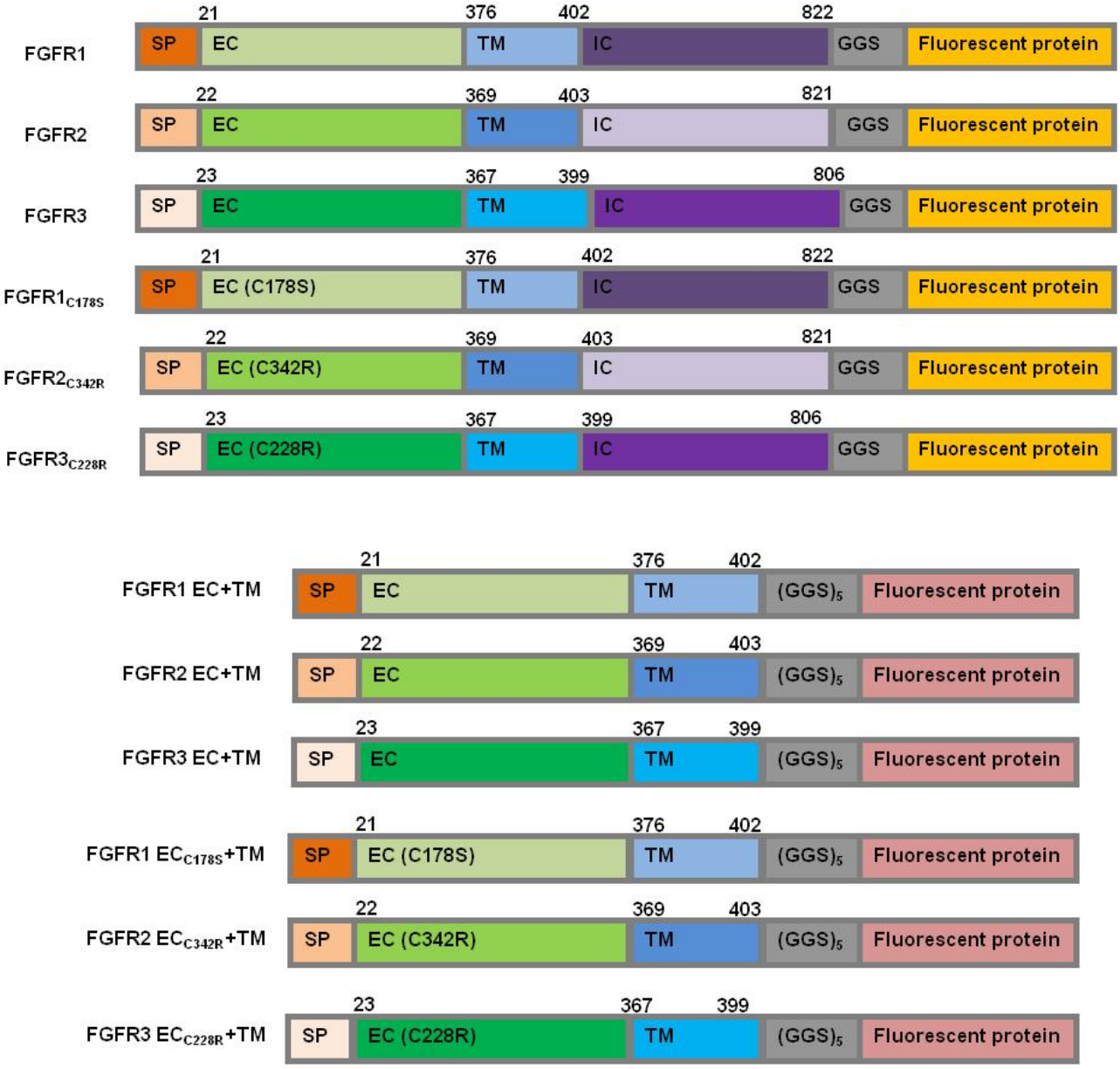

Figure S3. Plasmid constructs used in the FRET experiments. The full-length receptors had fluorescent proteins attached to their C-termini via a flexible GGS linker. The truncated receptors had the intracellular domain substituted with a fluorescent protein, which was attached to the TM domain via a longer flexible $(GGS)_5$ linker. SP: signal peptide, EC: extracellular domain, TM: transmembrane domain. Fluorescent protein was either YFP or mCherry (a FRET pair). Amino acid residue numbers are shown above the constructs.

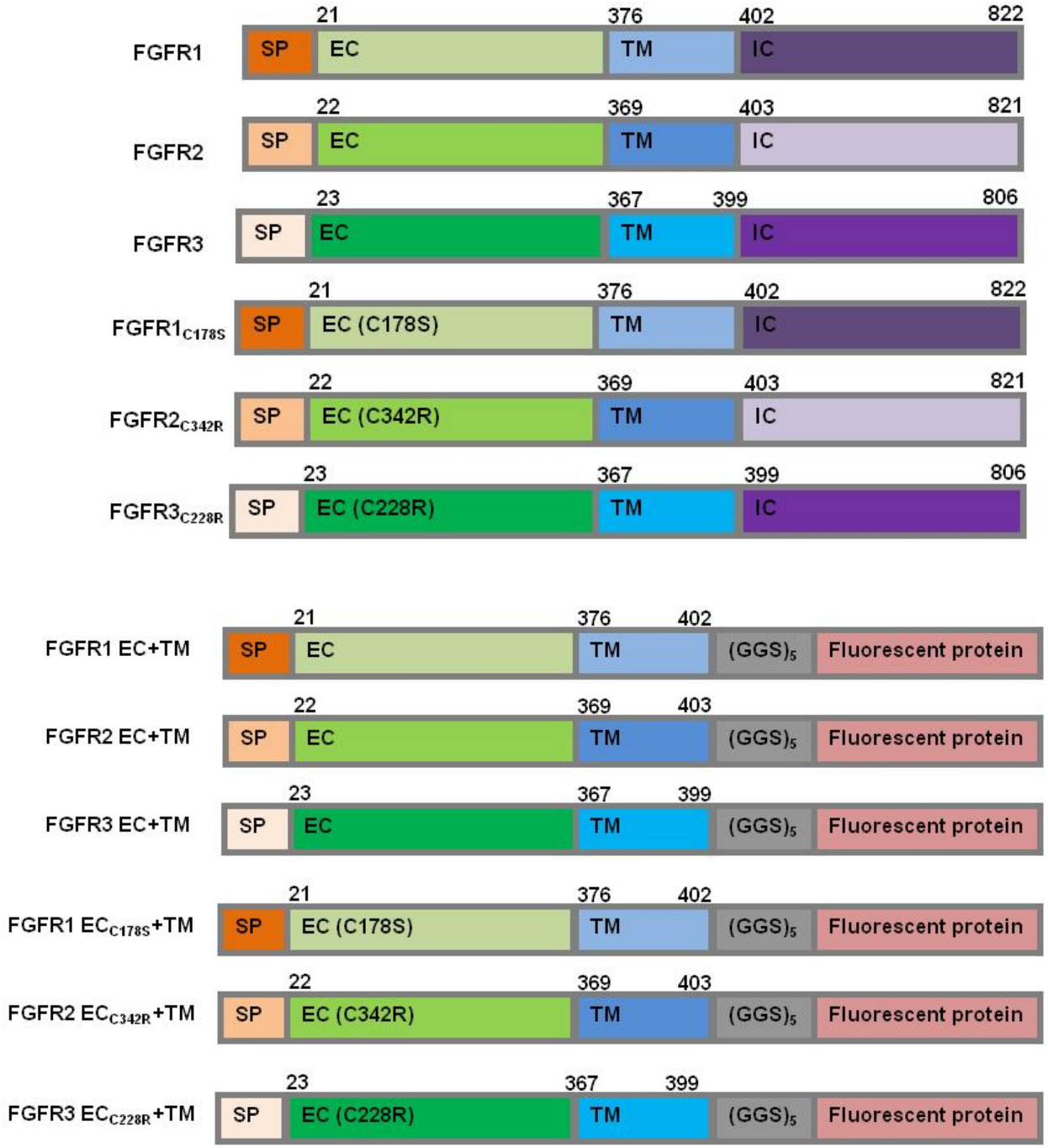

Figure S4. Plasmid constructs used for the Western blot experiments. Amino acid residue numbers are shown above the constructs.

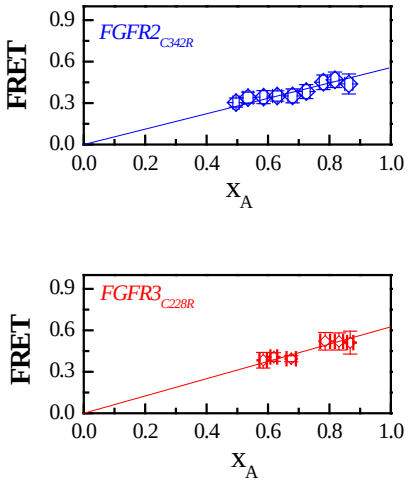

Figure S5. FRET as a function of receptor acceptor fraction. For constitutive oligomers, the FRET signal depends primarily on the acceptor fraction, $x_A=C_D/(C_D+C_A)$. The linear dependence is indicative of a dimer [14-16].

Reference List

1. Sarabipour, S. & Hristova, K. (2016). Mechanism of FGF receptor dimerization and activation. *Nat. Commun.* **7**, 10262.

2. Chen, L., Placone, J., Novicky, L. & Hristova, K. (2010). The extracellular domain of fibroblast growth factor receptor 3 inhibits ligand-independent dimerization. *Science Signaling* **3**, ra86.

3. Sarabipour, S. & Hristova, K. (2015). FGFR3 Unliganded Dimer Stabilization by the Juxtamembrane Domain. *J. Mol. Biol.* **427**, 1705-1714.

4. Sarabipour, S., Chan, R. B., Zhou, B., Di Paolo, G. & Hristova, K. (2015). Analytical characterization of plasma membrane-derived vesicles produced via osmotic and chemical vesiculation. *Biochim. Biophys. Acta* **1848**, 1591-1598.

5. Del Piccolo, N., Placone, J., He, L., Agudelo, S. C. & Hristova, K. (2012). Production of plasma membrane vesicles with chloride salts and their utility as a cell membrane mimetic for biophysical characterization of membrane protein interactions. *Anal. Chem.* **84**, 8650-8655.

6. Chen, L. R., Novicky, L., Merzlyakov, M., Hristov, T. & Hristova, K. (2010). Measuring the Energetics of Membrane Protein Dimerization in Mammalian Membranes. *J. Am. Chem. Soc.* **132**, 3628-3635.

7. Sarabipour, S., King, C. & Hristova, K. (2014). Un-induced high-yield bacterial expression of fluorescent proteins. *Anal. Biochem.* **449**, 155-157.

8. Li, E., Placone, J., Merzlyakov, M. & Hristova, K. (2008). Quantitative measurements of protein interactions in a crowded cellular environment. *Anal. Chem.* **80**, 5976-5985.

9. Wolber, P. K. & Hudson, B. S. (1979). An analytic solution to the Förster energy transfer problem in two dimensions. *Biophys. J.* **28**, 197-210.

10. Posokhov, Y. O., Merzlyakov, M., Hristova, K. & Ladokhin, A. S. (2008). A simple "proximity" correction for Forster resonance energy transfer efficiency determination in membranes using lifetime measurements. *Analytical Biochemistry* **380**, 134-136.

11. Snyder, B. & Freire, E. (1982). Fluorescence energy transfer in two dimensions. A numeric solution for random and nonrandom distributions. *Biophys. J.* **40**, 137-148.

12. King, C., Sarabipour, S., Byrne, P., Leahy, D. J. & Hristova, K. (2014). The FRET signatures of non-interacting proteins in membranes: simulations and experiments. *Biophys. J.* **106**, 1309-1317.

13. Sarabipour, S., Del Piccolo, N. & Hristova, K. (2015). Characterization of Membrane Protein Interactions in Plasma Membrane Derived Vesicles with Quantitative Imaging Forster Resonance Energy Transfer. *Acc. Chem. Res.* **48**, 2262-2269.

14. Li, M., Reddy, L. G., Bennett, R., Silva, N. D., Jr., Jones, L. R. & Thomas, D. D. (1999). A fluorescence energy transfer method for analyzing protein oligomeric structure: Application to phospholamban. *Biophys. J.* **76**, 2587-2599.

15. Adair, B. D. & Engelman, D. M. (1994). Glycophorin a helical transmembrane domains dimerize in phospholipid bilayers - a resonance energy transfer study. *Biochemistry* **33**, 5539-5544.

16. Schick, S., Chen, L. R., Li, E., Lin, J., Koper, I. & Hristova, K. (2010). Assembly of the M2 Tetramer Is Strongly Modulated by Lipid Chain Length. *Biophys. J.* **99**, 1810-1817.